

Analysis of BDS ARAIM Integrity Support Data Parameters

Changjiang Geng*¹ | Chenghe Fang¹ | Zhigang Hu² | Xiaoli Song¹ | Lei Chen³ |
Zhipeng Wang⁴ | Yilun Cui¹

¹ Beijing Research Institute of Telemetry,
Beijing, China

² GNSS Research Center, Wuhan
University, Wuhan, China

³ Beijing Institute of Tracking and
Telecommunication Technology, Beijing,
China

⁴ School of Electronic and Information
Engineering, Beihang University, Beijing,
China

Correspondence

Changjiang Geng
Beijing Research Institute of Telemetry,
Beijing, China,
Email: gengchangjiang@hotmail.com

Abstract

The realization of the advanced receiver autonomous integrity monitoring (ARAIM) algorithm relies on integrity support data (ISD). To support the use of the BeiDou Navigation Satellite System (BDS) in ARAIM applications, the ISD parameters for BDS are analyzed. Global averages and worst-case signal-in-space ranging errors (SISREs) are computed using data from July 2020 to July 2022. The data cover three open signals: B1I, B1C, and B2a, which are committed for civilian aviation uses. The complementary Gaussian cumulative distribution function is used to bound the SISREs of different signals for all satellites. The results show that the global SISRE values are less than 0.6 m (root mean square) for B1I, B1C, and B2a signals, and the worst-case SISRE can be bounded by a zero-mean Gaussian distribution with a standard deviation of 4.0 m at the 4.0×10^{-5} level. Furthermore, a general discussion of P_{const} and b_{nom} is presented, with some recommendations.

Keywords

ARAIM, BDS, bound, integrity support message

1 | INTRODUCTION

As first proposed by the Global Positioning System (GPS) Evolutionary Architecture Study and further developed by the United States–European Union working group, the advanced receiver autonomous integrity monitoring (ARAIM) technique has been developed for civil aviation. Different from the traditional receiver autonomous integrity monitoring (RAIM) algorithm, ARAIM works with integrity support data (ISD) from global navigation satellite system (GNSS) constellations and a user algorithm to obtain a positioning solution with a specified integrity and continuity level (WG-C, 2017). The user algorithm can be based on multiple-hypothesis solution separation or some other method. ARAIM was designed to realize the localizer performance with vertical guidance (LPV)-200 approach at a global scale using dual-frequency and multi-constellation observations. Simulation results show that the dual constellations of GPS and Galileo can provide smooth coverage for different requirements worldwide with specified ISD parameters (WG-C, 2015, 2016; Blanch et al., 2022).

In the development of ARAIM techniques, one of the most important tasks is to determine the ISD parameters related to signal-in-space (SIS) accuracy and integrity. A proven approach for an ISD generation algorithm has been developed,

which has been used for GPS and GLONASS ISD analysis (Perea et al., 2017; Walter et al., 2018). A similar method has been used to evaluate Galileo performance (Brieden et al., 2019; Wallner et al., 2021).

As a new navigation constellation, the BeiDou Navigation Satellite System (BDS) has been providing global services with third-generation satellites (BDS-3) since July 2020. The BDS-3 baseline constellation consists of 24 medium Earth orbit (MEO) satellites, three inclined geosynchronous satellite orbit (IGSO) satellites, and three geostationary Earth orbit satellites. BDS has committed to the International Civil Aviation Organization (ICAO) to provide open service through three signals, i.e., B1I, B1C, and B2a, with central frequencies of 1561.098, 1575.42, and 1176.45 MHz, respectively (Yang et al., 2020). The B1C and B2a signals have the same central frequency as GPS L1 and L5 and Galileo E1 and E5a, which brings benefits for the compatibility and interoperability of these three systems. With 24 MEO satellites transmitting B1C and B2a signals, BDS enhances the capability of L1- and L5-compatible dual-frequency user equipment and related applications.

To promote the use of the BDS in ARAIM applications, the ISD parameters of BDS must be analyzed. Although some studies have conducted a statistical characterization of the BDS signal-in-space ranging error (SISRE) (Lv et al., 2019; Chen et al., 2021), they concentrated on accuracy analysis. The integrity parameters used for BDS ARAIM applications have been preliminarily verified for the B1I signal of BDS-2 and BDS-3 satellites (Wang et al., 2021; Zhang et al., 2023; Wang et al., 2024), but the B1C and B2a signals have not been investigated. In this work, a comprehensive study of the ISD parameters of the BDS is conducted, the performance of the B1I, B1C, and B2a signals is analyzed, and an integrity analysis is provided based on precise satellite health data with a high sampling rate.

2 | DATA SOURCE

The data used in this study cover the period from July 2020 to July 2022. To ensure that the data are as precise as possible, broadcast ephemeris data from the global stations of the international GNSS Monitoring and Assessment System (iGMAS) (Birinci, 2023) and the International GNSS Service (IGS)(Johnston, 2017) are combined. The combined broadcast ephemeris can be downloaded from the China Satellite Navigation Office Test and Assessment Research Center (CSNO-TARC) website (www.csno-tarc.cn).

The BDS B1I signal is modulated with the D1 navigation message for MEO and IGSO satellites, whereas the B1C and B2a signals are modulated with the B-CNAV1 and B-CNAV2 navigation messages (CSNO, 2017a, 2017b, 2019). Because the parameters differ for D1 and B-CNAV1/B-CNAV2, an extended receiver independent exchange (RINEX) format is used for recording B-CNAV1/B-CNAV2 data at the iGMAS data center.

As a reference for evaluating SISREs, precise ephemeris and clock offsets play a key role in this work. We use precise ephemerides from the iGMAS and IGS analysis centers; specifically, the products from Wuhan University (WHU) and Helmholtz Centre Potsdam (GBM) are used for calculating the SISRE. The precise products are recorded at 5-min intervals. The following strategies are used to improve the precision and completeness of the evaluation:

- (1) Because only a small number of stations have B1C/B2a tracking capability, there is more abnormality in the recorded raw ephemeris for B-CNAV1 and B-CNAV2. To extract abnormal data, we compare the B-CNAV1/B-CNAV2

data with D1 data and remove any data that are inconsistent with D1, based on the reality that all of the ephemerides and clock offsets of different signals are fitted with the same orbit determination results at the BDS control segment. If two stations record the same incorrect ephemeris, the data should not be considered as abnormal, regardless of whether the data are inconsistent with D1.

- (2) The completeness of WHU precise products must be verified. If there are gaps or if the data record is invalid (when the satellite is in healthy mode, some records are lost through a large residual error during a fault event), GBM products or other products will be used.
- (3) If the SISREs exceed the integrity limit, we also assess the consistency of different precise ephemeris products, to avoid a misleading alarm for an integrity check.
- (4) If data are missing for all of the products and the status of the navigation signal is set to “healthy” at that time, PANDA software is used to reprocess those global observables to obtain a precise orbit and clock offset (Zhao et al., 2022).

Health data represent an important data source in this work and are sampled at 1-min intervals. As the health flag in the navigation message of different signals can change any time that the SISRE exceeds the limit specified by the control segment and the widely used RINEX-format ephemeris may only record the health flag with an ephemeris update interval (1 h for BDS), we cannot use health data from RINEX broadcast ephemeris files to obtain the precise fault time, as this would not include a precise alarm time. At iGMAS stations, we record the navigation signal health flag with a 1-min interval in a separate file. We also compare these data with the injection records of the control segment to ensure the accuracy of this data source.

3 | DEFINITION AND METHODOLOGY

As defined in the ARAIM concept, at least seven ISD parameters will be directly utilized by the dual-frequency user algorithm: σ_{URE} , σ_{URA} , b_{nom} , P_{sat} , P_{const} , R_{sat} (or MFD_{sat}), and R_{const} (or MFD_{const}). Definitions of these parameters are listed in Table 1 (WG-C, 2016).

TABLE 1
Definitions of ISD Parameters

No.	Parameter	Definition
1.	σ_{URE}	Standard deviation of SISRE for any satellite used for accuracy and continuity
2.	σ_{URA}	Standard deviation of SISRE for any satellite used for integrity
3.	b_{nom}	Maximum nominal bias for any satellite used for integrity
4.	P_{sat}	Probability that an individual satellite is in a faulted state at any given time
5.	P_{const}	Probability that multiple satellites are in a faulted state at any given time
6.	R_{sat}	Fault rate of an individual satellite
7.	R_{const}	Fault rate of multiple satellites
8.	MFD_{sat}	Mean fault duration of an individual satellite
9.	MFD_{const}	Mean fault duration of multiple satellites

3.1 | Instantaneous SISRE

To evaluate ISD parameters, the SISRE must be precisely estimated. σ_{URE} is a direct statistic of the instantaneous SISRE, with σ_{URA} serving as a bound. There are several methods for calculating the instantaneous SISRE of a specified satellite. One commonly used method is based on the globally averaged instantaneous SISRE (AVE SISRE), which takes a weighted average of the orbital errors projected onto the Earth's surface (Heng et al., 2012; Montenbruck et al., 2018). The generalized effects of orbit and clock errors on all users of the Earth's surface can be well represented. The AVE SISRE is defined as follows:

$$AVE\ SISRE = \sqrt{(\alpha R - T)^2 + \beta(A^2 + C^2)} \quad (1)$$

Here, R, A, C are the orbital errors of the broadcast ephemeris in the radial, along-track, and cross-track directions, respectively. T is the error of the broadcast clock offset converted to length, and α and β are factors related to the satellite orbital height, which are set to 0.9823 and 0.1324 for BDS MEO satellites.

Another method is based on the instantaneous SISRE at the worst user location (WUL SISRE, also known as worst-case SISRE), which corresponds to the maximum value of all SISREs projected to every user location on the Earth's surface with a specified elevation mask (5° is used in this work). This problem can be converted to a two-dimensional problem that consists of identifying the plane that contains the center of the Earth and the vector of the orbital error and then projecting the orbit error vector to determine the maximum SISRE value (Heng et al. 2012; Perea et al., 2017). The method for computing the WUL SISRE can be expressed as follows:

$$WUL\ SISRE = \max(|ISISRE_i|) * \text{sign}(ISISRE_i) \quad (2)$$

where $ISISRE_i$ is the sum of the orbital and clock offset errors. The orbital error is the length of its vector projected to the user's line of sight in accordance with different users' locations on Earth.

For SISRE analysis, the AVE SISRE method obtains more correct SISRE information on accuracy; in contrast, for integrity-related purposes, the WUL SISRE bound can ensure better integrity. Thus, in this work, we use the AVE SISRE for σ_{URE} calculation and the WUL SISRE for σ_{URA} , P_{sat} , and P_{const} analysis.

In both methods, antenna phase center offsets must be corrected for orbital error calculations, as the precise orbit takes the satellite's center of mass as a reference, whereas the broadcast ephemeris uses the antenna phase center. The antenna phase center of BDS satellites can be downloaded from the CSNO-TARC website (<https://www.csno-tarc.cn/en/datacenter/satelliteparameters>). Additionally, because the references for the precise clock offset and broadcast clock offset are different, these terms need to be aligned to the same reference for comparison (Montenbruck et al., 2018). Moreover, the precise ephemeris is obtained from ionosphere-free combination observations, whereas the broadcast clock offset refers to the B3I signal for BDS. Thus, the influence of the timing group delay (TGD) must be considered for evaluating the accuracy of the broadcast clock offset (Lv et al., 2019). In this work, the broadcast TGD data are used for correcting the code bias between different signals.

3.2 | Fault Identification

A fault event indicates that the SISRE of a satellite is larger than the specified error threshold, but the system fails to issue warning information in a timely

manner. The warning information here refers to the “unhealthy” flag in navigation messages. Hence, two conditions must be met to determine a fault for a navigation signal: first, the satellite is flagged as “healthy”; second, the satellite SISRE exceeds the error threshold. For integrity, the error threshold can be represented as follows:

$$H = \kappa \cdot \sigma_{URA} \quad (3)$$

Here, H is the SISRE threshold for fault identification, whereas κ is a multiplier for ensuring that the threshold is met with a specified confidence level.

For the B1I signal, the method for judging the “health” of a satellite is relatively simple, based on only the “SatH1” flag in the D1 navigation message; in contrast, for B1C and B2a signals, this judgment requires an integration of the status of four parameters (health status (HS), signal integrity flag (SIF), data integrity flag (DIF), and accuracy integrity flag (AIF)) in the B-CAV1/B-CAV2 navigation message (CSNO, 2017a, 2017b, 2019).

In addition, the user range accuracy (URA)/signal-in-space accuracy are broadcasted in BDS navigation messages, but these parameters are not currently designed for ARAIM. Therefore, we compute the WUL SISRE statistic for all satellites and obtain an overbound at a specified probability level using a zero-mean Gaussian distribution. The specified probability level corresponds to κ times the specified standard deviation.

4 | ANALYSIS RESULTS FOR ISD PARAMETERS

4.1 | SISRE Standard Deviation

AVE SISRE statistics of the B1I signal for all satellites are shown in Figure 1. It can be seen that all satellites except pseudorandom noise (PRN) 27 have a median AVE SISRE of less than 1.0 m.

The mean AVE SISRE for all satellites is 0.58 m. Satellite PRN27 has the largest error, 1.2 m, among all satellites. By assessing the orbit and clock errors of this satellite (Figure 5), we found that there was a larger deviation in the clock offset error of this satellite. That error is most likely caused by signal deformation and other error sources, which requires further study.

Although different ephemeris parameters are used (the new B-CAV1 and B-CNAV2 ephemerides have two additional parameters: the change rate of the semi-major axis and the mean motion difference)(CSNO, 2017a, 2017b), the ephemerides modulated on the B1C and B2a signals are generated from the same orbit

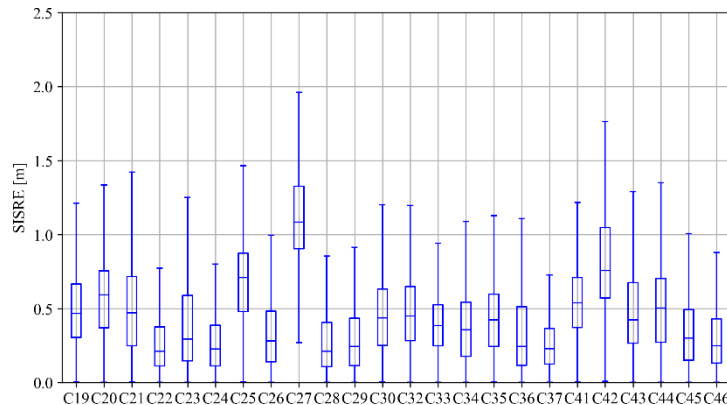


FIGURE 1 Boxplot of the B1I AVE SISRE for different satellites

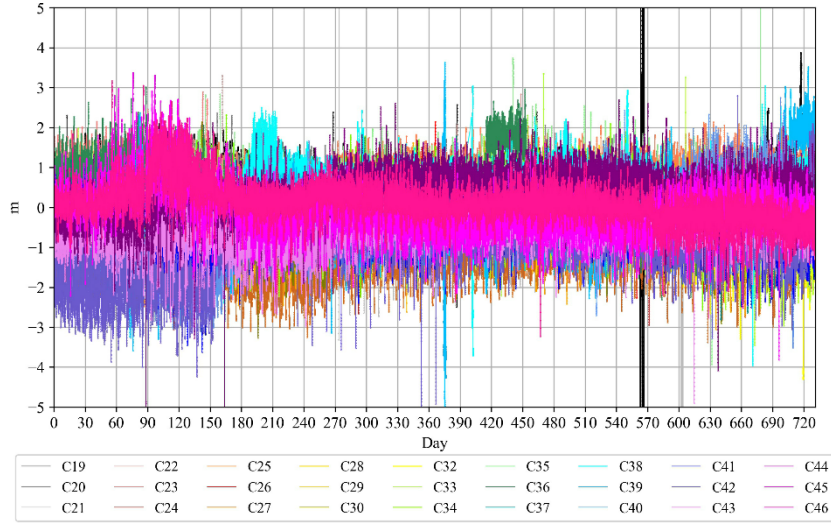


FIGURE 2 BII WUL SISRE time series for all satellites

determination results obtained for the B1I signal. The mean AVE SISRE value for the B1C and B2a signals is 0.57 m, showing an improvement of several centimeters compared with the B1I value (a figure of the B1C/B2a AVE SISRE is not shown here).

The WUL SISRE of the B1I signal is shown in Figure 2. Unlike the AVE SISRE, the WUL SISRE has positive and negative values, which can be clearly expected from a comparison of Equations (1) and (2). In general, because the error caused by orbital deviation in the AVE SISRE is primarily affected by deviations in the radial direction, the basic change characteristics of the WUL SISRE and AVE SISRE are similar. Furthermore, because more parameters are used in the B-CNAV1 and B-CNAV2 ephemerides, the WUL SISRE of the B1C and B2a signals is slightly better than that of the B1I signal, with a centimeter-level difference. The heavy black line at day 565 shows a fault event for the PRN19 satellite, which will be clarified in Section 4.4.

4.2 | Overbounding the SISRE

There are several methods for error bounding (Walter et al., 2018; Wang et al., 2021; Martini et al., 2020). In this work, we use the one minus Gaussian cumulative distribution function (1-CDF) method to overbound the absolute value of the WUL-SISRE for all satellites. The 1-CDF overbounding can be expressed as shown in Equation (4), where Φ is the Gaussian cumulative distribution function (CDF), Φ_o is the overbounding CDF, and Φ_a is the actual CDF:

$$1 - \Phi_o(|x|) \geq 1 - \Phi_a(|x|) \quad (4)$$

As the faults in different satellites can equally affect all satellites, it is reasonable to aggregate the data for all satellites and use the average fault probability for bounding analysis (Walter et al., 2019). Figure 3 shows the 1-CDF curve for WUL SISRE aggregation of all satellites. It can be seen that the WUL SISRE for all satellites (after subtracting the mean value for each satellite) can be overbounded by a zero-mean Gaussian distribution with a standard variation of 4.0 m at a probability level of 4.0×10^{-5} .

Figure 4 shows 1-CDF curves for individual satellites (colored lines). It can be seen that the curves for PRN19 (blue), PRN21 (purple), and PRN44 (green) intersect the expected bounding line. This result indicates that these three satellites do not fulfill the specified integrity requirement. An analysis of the faults for these satellites is presented in Section 4.4.

4.3 | Nominal Bias

A determination of b_{nom} should consider orbit and clock offset biases, TGD error, satellite antenna biases, signal distortion, and other errors (Walter et al., 2018).

For orbital and clock offset errors, the probability distribution function of the WUL SISRE (Figure 5) shows that the orbital deviation basically exhibits the characteristics of zero mean in all directions; however, the clock offset error obviously has a bias, and its magnitude varies for different satellites. The satellite with the largest SISRE (PRN27) has the largest bias, with a value of -1.16 m. This bias would be considered as the main source of b_{nom} in BDS applications. The composition of that bias would be complex. If we use precise TGD to evaluate the broadcast clock

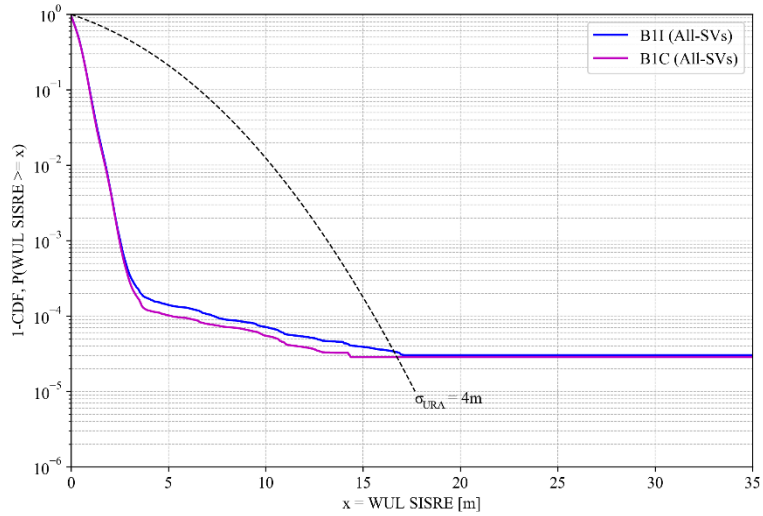


FIGURE 3 Overbounding the WUL SISRE aggregation for all satellites

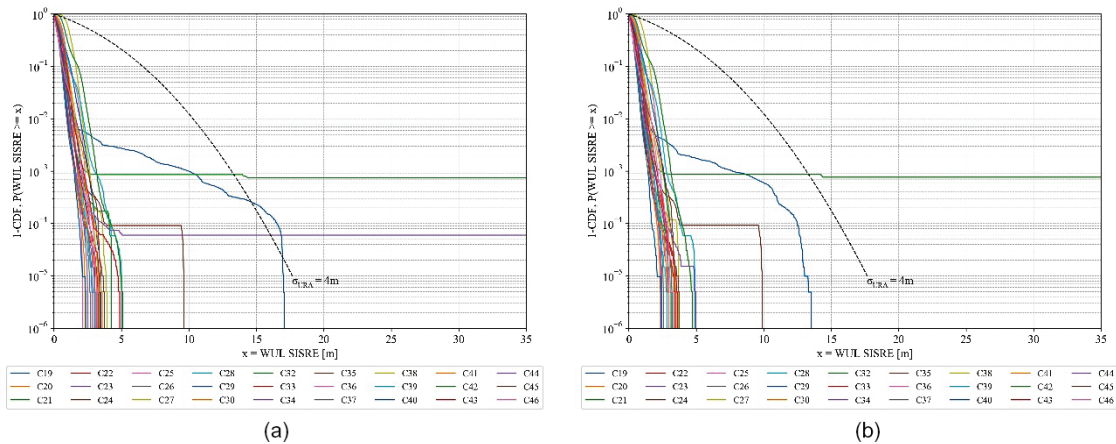


FIGURE 4 Overbounding the WUL SISRE for individual satellites (a) B1I (b) B1C/B2a

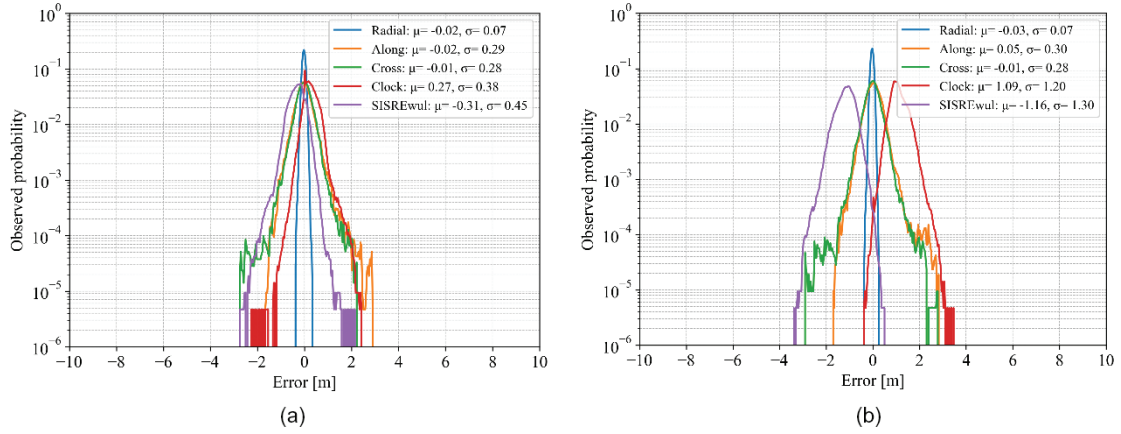


FIGURE 5 Orbit and clock offset errors and the WUL SISRE probability density function (a) PRN26 (b) PRN27

offset, the result would be improved. The remaining error may be introduced by the different tracking modes of the control segment and the commercial receivers used here (Chen et al., 2021). Additionally, signal distortion would also exacerbate this bias.

For TGD errors, because the broadcast clock offset of BDS is not calculated from an ionosphere-free combination of dual-frequency observations (it refers to the B3I signal), the TGD should be considered in BDS dual-frequency positioning. The impact of TGD on dual-frequency combination observation can be expressed as follows:

$$b_{ca} = \frac{f_c^2}{f_c^2 - f_a^2} b_c - \frac{f_a^2}{f_c^2 - f_a^2} b_a \quad (5)$$

where b is the TGD for a single signal, f is the frequency of the carrier phase, and the subscripts c a indicate the B1C and B2a signals. Previous work has shown that the BDS TGD has an accuracy of approximately 1.0 ns when the bias between the broadcast TGD and the IGS differential code bias (DCB) is removed, if the IGS DCB is taken as a reference for TGD evaluation (Wang et al., 2019).

For satellite antenna bias, except the fixed antenna phase center offset, the variation in the antenna phase center is on order of millimeters (Hu et al., 2022), and the effect on b_{nom} is small.

With regard to the impact of signal distortion, a well-designed receiver can achieve a pseudorange deviation within 0.2 m (He et al., 2020). This result is dependent on the receiver design (Hauschild & Montenbruck, 2016; Gong et al., 2022).

To summarize the above results, considering that the impacts of signal distortion and TGD have already been included in the evaluated SISRE, we simplify this analysis by setting the nominal bias of the BDS to 1.16 m. However, much work is still needed to characterize the effects of these biases and to determine their bounds. There exist more error sources such as antenna bias, code-carrier incoherence, and DCB for the receiver side (Walter et al., 2018), which require an in-depth study.

4.4 | Fault Rate and Probability

While determining σ_{URA} to overbound the actual SISRE distribution in the prior section, we also obtain the corresponding probability level, parameter P_{sat} .

TABLE 2
Fault Events During the Studied Time Period

No.	Satellite	Start Time (BDT)	End Time (BDT)	Affected Signals
1	PRN19	2022-02-17 18:55	2022-02-17 20:39	B1I
2	PRN21	2022-03-25 16:00	2022-03-26 04:39	B1I/B1C/B2a
3	PRN44	2021-01-10 22:00	2021-01-10 23:00	B1I

According to the WUL SISRE bounding analysis, P_{sat} is set to 4.0×10^{-5} , corresponding to a bounding σ_{URA} of 4.0 m. The corresponding κ for a cumulative probability of 4×10^{-5} is approximately 4.1, which can be used for assessing fault events. Three fault events were found for the B1I signal, with only one fault event for the B1C and B2a signals (listed in Table 2). Consequently, R_{sat} would be 7.1×10^{-6} for the B1I signal and 2.4×10^{-6} for the B1C and B2a signals.

For P_{const} , it is obvious that there are no cases in which two or more satellites are interrupted simultaneously during the studied time period. The value of 6.0×10^{-5} , which was suggested in the ICAO Standard and Recommended Practices (ICAO, 2023), may be conservative (indicating that one fault happens in 2 years, corresponding to an R_{const} value of $5.7 \times 10^{-5}/h$). One should note that the data set used in this analysis is limited; a longer-term data set is needed to obtain more precise results.

5 | CONCLUSION

ARAIM technology shows great potential for safety-related applications. The BDS has L1/L5 dual-band navigation signal (B1C and B2a) service capability with 24 satellites, which can support ARAIM dual-frequency applications. Accurate and in-depth analyses of the ISD parameters are needed for applying BDS signals to ARAIM.

In this work, we analyzed the ISD parameters of BDS satellites for ARAIM, i.e., σ_{URE} , σ_{URA} , b_{nom} , P_{sat} , P_{const} , R_{sat} , and R_{const} . The data cover the period from July 2020 to July 2022. In addition to B1I, the performance of the new B1C and B2a signals was analyzed. The results show that the σ_{URE} value of BDS (global average) is less than 0.6 m (root mean square) and that the worst-case SISRE can be well overbounded by a zero-mean Gaussian distribution with a standard deviation of 4.0 m at a level of 4×10^{-5} . Thus, a value of 4.0 m is recommended for σ_{URA} , with a P_{sat} value of 4×10^{-5} and a b_{nom} value of 1.16 m, whereas a P_{const} value of 6.0×10^{-5} is recommended, as no more than two satellites exhibited faults at the same time during the evaluation period.

REFERENCES

- Birinci, S., & Saka, M. H. (2023). Sub-meter-level navigation with an enhanced multi-GNSS single-point positioning algorithm using iGMAS ultra-rapid products. *The Journal of Navigation*, 76(1), 133–151. <https://doi.org/10.1017/S0373463322000601>
- Blanch, J., Walter, T., Milner, C., Joerger, M., Pervan, B., & Bouvet, D. (2022). Baseline advanced RAIM user algorithm: Proposed updates. *Proc. of the 2022 International Technical Meeting of the Institute of Navigation*, Long Beach, CA, 229–251. <https://doi.org/10.33012/2022.18254>
- Brieden, P., Wallner, S., Canestri, E., Joly, D., Subirana, J. S., Martini, I., Nuckelt, A., Battista, G., Lauria, D., Luongo, F., Cosson, F., Merlan, N. C., Baur, O., Lieb, V., Odriozola, M., Spinelli, E., Alonso, M. T., Rovira-Garcia, A., Alcantarilla, I., & Kirchner, M. (2019). Galileo characterization as input to H-ARAIM and SBAS DFMC. *Proc. of the 32nd International Technical Meeting of the Satellite Division of the Institute of Navigation (ION GNSS+ 2019)*, Miami, FL, 2819–2841. <https://doi.org/10.33012/2019.16922>

- Chen, G., Zhou, R., Hu, Z., Lv, Y., Wei, N., & Zhao, Q. (2021). Statistical characterization of the signal-in-space errors of the BDS: A comparison between BDS-2 and BDS-3. *GPS Solutions*, 25(3), 112. <https://doi.org/10.1007/s10291-021-01150-x>
- CSNO. (2017a). *BeiDou Navigation Satellite System signal in space interface control document: Open service signal B1C* (Version 1.0). <http://m.beidou.gov.cn/xt/gfzx/201712/P020171226741342013031.pdf>
- CSNO. (2017b). *BeiDou Navigation Satellite System signal in space interface control document: Open service signal B2a* (Version 1.0). <http://www.beidou.gov.cn/xt/gfzx/201712/P020171226742357364174.pdf>
- CSNO. (2019). *BeiDou Navigation Satellite System signal in space interface control document: Open service signal B1I* (Version 3.0). <http://en.beidou.gov.cn/SYSTEMS/ICD/201902/P020190227702348791891.pdf>
- Gong, X., Zheng, F., Gu, S., Zhang, Z., & Lou, Y. (2022). The long-term characteristics of GNSS signal distortion biases and their empirical corrections. *GPS Solutions*, 26(2), 52. <https://doi.org/10.1007/s10291-022-01238-y>
- Hauschild, A., & Montenbruck, O. (2016). The effect of correlator and front-end design on GNSS pseudorange biases for geodetic receivers. *NAVIGATION*, 63(4), 443–453. <https://doi.org/10.1002/navi.165>
- He, C., Lu, X., Guo, J., Su, C., Wang, W., & Wang, M. (2020). Initial analysis for characterizing and mitigating the pseudorange biases of BeiDou Navigation Satellite System. *Satellite Navigation*, 1(1), 3. <https://doi.org/10.1186/s43020-019-0003-3>
- Heng, L., Gao, G. X., Walter, T., & Enge, P. (2012). GPS signal-in-space integrity performance evolution in the last decade. *IEEE Transactions on Aerospace and Electronic Systems*, 48(4), 2932–2946. <https://doi.org/10.1109/TAES.2012.6324670>
- Hu, Z., Cai, H., Jiao, W., Zhou, R., Zhai, Q., Liu, X., Kan, H., & Zhao, Q. (2022). Preliminary results of iGMAS BDS/GNSS absolute antenna phase center field calibration. In *China Satellite Navigation Conference (CSNC 2022) Proceedings: Lecture Notes in Electrical Engineering*, Vol. 910, 147–160. Springer Nature. https://doi.org/10.1007/978-981-19-2576-4_13
- International Civil Aviation Organization (ICAO). (2023). *International standards and recommended practices annex 10*. <https://eur-lex.europa.eu/legal-content/EN/TXT/PDF/?uri=CELEX:52023PC0070>
- Johnston, G., Riddell, A., & Hausler, G. (2017). The International GNSS Service. In P. J. G. Teunissen & O. Montenbruck (Eds.), *Springer handbook of global navigation satellite systems*, 1st ed., 967–982. Springer International Publishing. <https://doi.org/10.1007/978-3-319-42928-1>
- Lv, Y., Geng, T., Zhao, Q., Xie, X., & Zhou, R. (2019). Initial assessment of BDS-3 preliminary system signal-in-space range error. *GPS Solutions*, 24(1), 16. <https://doi.org/10.1007/s10291-019-0928-x>
- Martini, I., Sgammini, M., & Boyero, J. P. (2020). Error bounding for ARAIM integrity support message generation. *Proc. of the 33rd International Technical Meeting of the Satellite Division of the Institute of Navigation (ION GNSS+ 2020)*, 1068–1088. <https://doi.org/10.33012/2020.17577>
- Montenbruck, O., Steigenberger, P., & Hauschild, A. (2018). Multi-GNSS signal-in-space range error assessment – methodology and results. *Advances in Space Research*, 61(12), 3020–3038. <https://doi.org/10.1016/j.asr.2018.03.041>
- Perea, S., Meurer, M., Rippl, M., Belabbas, B., & Joerger, M. (2017). URA/SISA analysis for GPS and Galileo to support ARAIM. *NAVIGATION*, 64(2), 237–254. <https://doi.org/10.1002/navi.199>
- Wallner, S., Perea, S., Odriozola, M., Brieden, P., Binder, K., Nuckelt, A., Donatelli, A., Joly, D., Stallo, C., Sgammini, M., Martini, I., Boyero, J. P., Mabilieu, M., & Canestri, E. (2021). Galileo H-ARAIM characterization and Galileo integrity support message (ISM). *Proc. of the 34th International Technical Meeting of the Satellite Division of the Institute of Navigation (ION GNSS+ 2021)*, St. Louis, MO, 1375–1391. <https://doi.org/10.33012/2021.18153>
- Walter, T., Blanch, J., & Gunning, K. (2019). Standards for ARAIM ISM data analysis. *Proc. of the ION 2019 Pacific PNT Meeting*, Honolulu, HI, 777–784. <https://doi.org/10.33012/2019.16837>
- Walter, T., Gunning, K., Phelts, R. E., & Blanch, J. (2018). Validation of the unfaulted error bounds for ARAIM. *NAVIGATION*, 65(1), 117–133. <https://doi.org/10.1002/navi.214>
- Wang, N., Li, Z., Montenbruck, O., & Tang, C. (2019). Quality assessment of GPS, Galileo and BeiDou-2/3 satellite broadcast group delays. *Advances in Space Research*, 64(9), 1764–1779. <https://doi.org/10.1016/j.asr.2019.07.029>
- Wang, R., & Walter, T. (2024). Performance characterization of the BeiDou-3 constellation. *Proc. of the ION 2024 Pacific PNT Meeting*, Honolulu, HI, 81–93. <https://doi.org/10.33012/2024.19669>
- Wang, S., Zhai, Y., & Zhan, X. (2021). Characterizing BDS signal-in-space performance from integrity perspective. *NAVIGATION*, 68(1), 157–183. <https://doi.org/10.1002/navi.409>
- WG-C. (2015). *Working Group C - ARAIM technical subgroup: Milestone 2 report*. <https://www.gps.gov/policy/cooperation/europe/2015/working-group-c/ARAIM-milestone-2-report.pdf>
- WG-C. (2016). *Working Group C - ARAIM technical subgroup: Milestone 3 report*. <https://www.gps.gov/policy/cooperation/europe/2016/working-group-c/ARAIM-milestone-3-report.pdf>

- WG-C. (2017). *WG-C advanced RAIM technical subgroup reference airborne algorithm description document*. https://web.stanford.edu/group/scpnt/gpslab/website_files/maast/ARAIM_TSG_Reference_ADD_v3.0.pdf
- Yang, Y., Mao, Y., & Sun, B. (2020). Basic performance and future developments of BeiDou global navigation satellite system. *Satellite Navigation*, 1(1), 1. <https://doi.org/10.1186/s43020-019-0006-0>
- Zhang, H., Yiping Jiang, & Yang, L. (2023). Preliminary analysis of BDS-3 performance for ARAIM. *NAVIGATION*, 70(1). <https://doi.org/10.33012/navi.553>
- Zhao, Q., Guo, J., Wang, C., Lyu, Y., Xu, X., Yang, C., & Li, J. (2022). Precise orbit determination for BDS satellites. *Satellite Navigation*, 3(1). <https://doi.org/10.1186/s43020-021-00062-y>

How to cite this article: Geng, C., Fang, C., Hu, Z., Song, X., Chen, L., Wang, Z., & Cui, Y. (2025). Analysis of BDS ARAIM integrity support data parameters. *NAVIGATION*, 72(3). <https://doi.org/10.33012/navi.712>